

Investigating the Conditions of Automatic Assembly of Polyhedral Joints

Mikhail Vladimirovich Vartanov

Moscow Polytech University

Zinina Inna Nikolaevna

Moscow Polytech University

Klimenko Irina Leontievna

Moscow Polytech University

Tran Dinh Van (✉ trandinhvan1221@gmail.com)

Moscow Polytech University

Research Article

Keywords: the robotic assembly, the adaptive gripper, the vibration device, the mathematical model

Posted Date: December 8th, 2021

DOI: <https://doi.org/10.21203/rs.3.rs-1130198/v1>

License: © ⓘ This work is licensed under a Creative Commons Attribution 4.0 International License.

[Read Full License](#)

Investigating the conditions of automatic assembly of polyhedral joints

¹ *Mikhail Vladimirovich Vartanov, Faculty of Mechanical Engineering, Moscow Polytech University, Moscow, 107023, Russia, m.v.vartanov@mospolytech.ru*

² *Zinina Inna Nikolaevna, Faculty of Mechanical Engineering, Moscow Polytech University, Moscow, 107023, Russia, zin_ina@mail.ru*

³ *Klimenko Irina Leontievna, Faculty of Basic Competencies, Moscow Polytech University, Moscow, 107023, Russia, llk58@mail.ru*

⁴ *Tran Dinh Van, Faculty of Mechanical Engineering, Moscow Polytech University, Moscow, 107023, Russia, trandinhvan1221@gmail.com*

Abstract

Purpose – Providing the technological reliability of the robotic assembly of joints with RK-profile on the basis of adaptation devices and low-frequency oscillations.

Design/methodology/approach – Ensuring the assembly conditions is achieved by the vibration device that provides oscillations relative to the two axes, perpendicular to the assembly direction and rotation about the assembly axis. Compensation of the linear error in the position of the parts is attained by an adaptive gripper with a flexible link.

Findings – A mathematical model describing the assembly process of parts relative to the non-inertial coordinate system is developed. The technological modes of profile parts assembly are defined.

Originality/value – The robotic assembly method of profile joints by the adaptation devices, namely a combination of elastic fixing of the installed profile part and the simultaneous rotation and vibration of the base part to improve the process reliability is developed. Experimental studies confirmed the adequacy of the created mathematical model. The patent for the assembly method of profile joints with a gap is received.

Keywords the robotic assembly, the adaptive gripper, the vibration device, the mathematical model

Paper type Research paper

1. Introduction

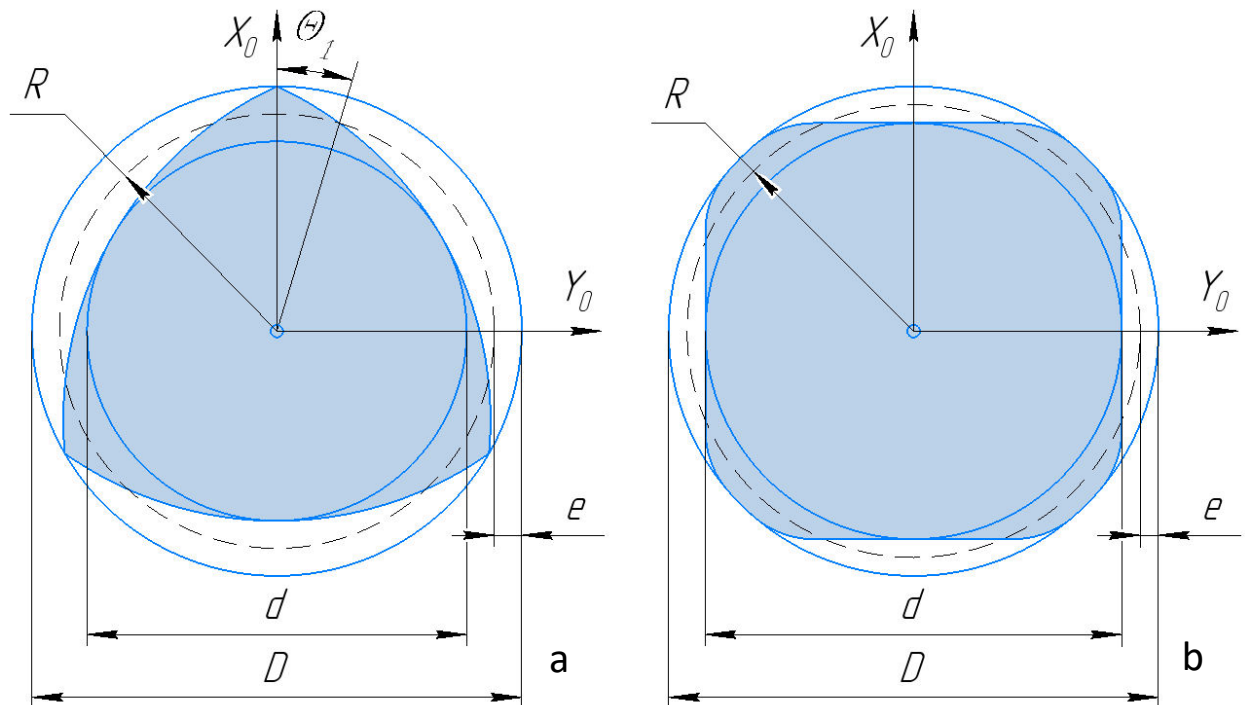
In the thirties of the last century the Austrian engineer E. Krause (Mossdorf, 1938) proposed the forming process of a cycloidal profile joint. The company Ernst Krause & Co AG produced machines for edge cutting and grinding machining of cycloidal profiles, so-called K-profiles.

Deeper research of the generation of geometry of external and internal K-profiles by turning and grinding, as well as their geometrical and service properties were carried out in the forties and sixties of the XX century R. Musyl (Musyl, 1946) and N.M. Karelin (Karelin, 1966). Disadvantages of these fabrication processes (a nonuniform angular velocity of the workpiece, the kinematics complexity of the machine, the low precision, etc.) prevented their widespread introduction into the industry.

Difficulties in improving the fabrication of cycloidal profile surfaces forced German engineers R. Musyl & F. Danzer (Musyl & Danzer, 1941) to develop a new form (called RK-profile) of the shaft and bush cross section curve and the process of its fabrication in 1941. The essence of this process is that two harmonic translational rectilinear motions (along the vertical Y and horizontal X coordinate axes) with a frequency N times higher than the speed of the workpiece are imparted to a cutting tool.

In mechanical engineering RK-profile joints are used in gearboxes and change gear boxes of turning and milling machines, in flexible modular tool systems, forge and press equipment, compressors and car gearboxes. RK-profile joints are mainly designed for transmitting torsion torque by conjugated surfaces of machine parts, cutting and auxiliary tools. They are used instead of splined and keyed joints.

RK and K –profile joints are characterized by the following geometric parameters (fig.1 a и b):



D – the diameter of the circumscribed circle; d – the diameter of the inscribed circle; $D_{PK} = 2R$ – the diameter of the middle circle (R – the radius of the middle circle); θ_1 – the angular parameter; e – the profile eccentricity; N – the number of faces.

Fig. 1. The geometric parameters of the profile shaft: a - RK-3, b – K-4

The surface equation of the RK-profile shaft is the following (Timchenko, 1993)

$$r_0(\theta_1) = \begin{pmatrix} [R - e \cdot \cos(N \cdot \theta_1)] \cdot \cos \theta_1 - N \cdot e \cdot \sin(N \cdot \theta_1) \cdot \sin \theta_1 \\ [R - e \cdot \sin(N \cdot \theta_1)] \cdot \sin \theta_1 + N \cdot e \cdot \cos(N \cdot \theta_1) \cdot \cos \theta_1 \\ z \\ 1 \end{pmatrix} \quad (1)$$

Joints with three faces have the property of automatic centering under a transmitted load at a certain clearance. The RK-profile joints can be with a guaranteed clearance or interference, with the transition fit. They can be cylindrical and conical (Timchenko, 1993).

Profile joints have a number of service and technological advantages over splined and keyed ones. The service properties include: the fatigue strength of the profile shaft is 4-5 times as much as the splined one; the running-in wear of the RK - 3 profile joints parts is 2,5-3 times, their torsional stiffness is 1,3-1,6 times, but the intensity of the steady-state wear is 1,8-2,4 times less. The profile joints such as PK-3 have the property of automatic centering under the transmitted load.

Currently, profile joints for the manufacture of drive shafts for cars and agricultural machinery are being extensively used, for instance “Weasler Engineering Inc.” (West Dend, Wisconsin, USA) and Bondioli & Pavesi S. p. A. (Italy) offers several modifications of profile drive shafts (fig. 2).

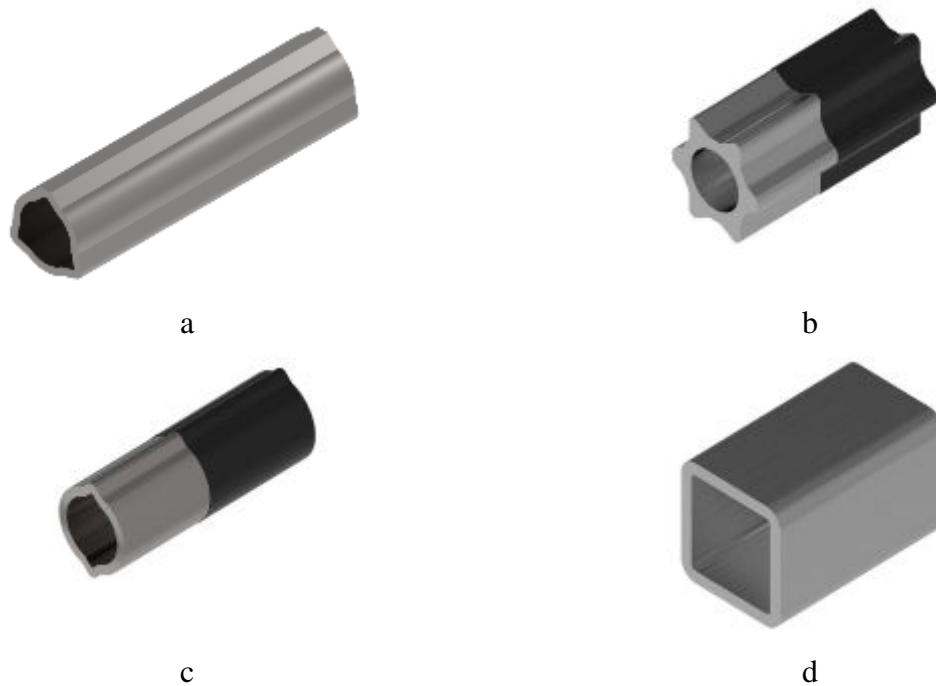


Fig. 2. Weasler’s profile pipes for drive shafts: a) trilobe profile tube; b) star profile tube; c) lemon profile tube; d) square tube

The feature of profile joints assembly is to achieve accuracy towards six coordinates - three linear and three angular ones (Fig.3). Permissible errors are determined in terms of the assembly process without jamming parts. In general, the task is to meet the following conditions:

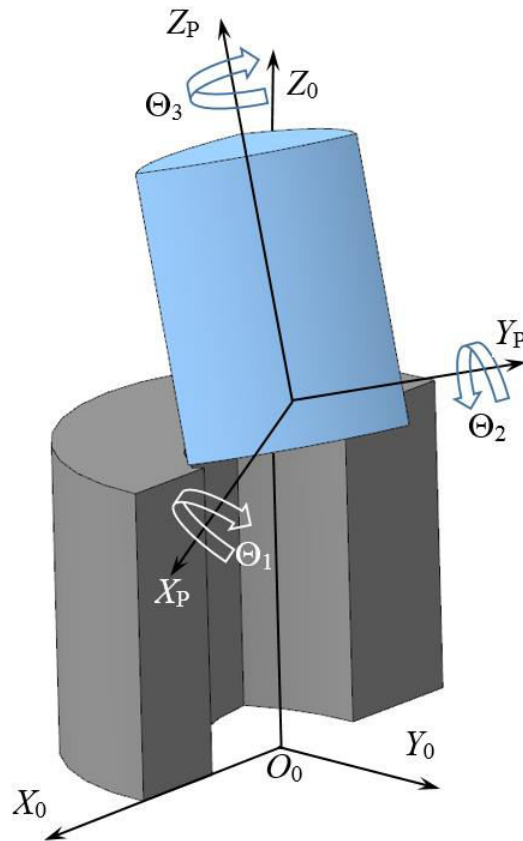


Fig.3. Problem statement of ensuring accuracy at the assembly position: a – the problem of spatial alignment; b – (origin of) an error when aligning assembled parts

$$\begin{aligned} \delta_{\Sigma} &\leq [\delta_0]; \\ \varphi_{\Sigma} &\leq [\varphi_0]; \\ \gamma_{\Sigma} &\leq [\gamma_0] \end{aligned} \quad (2)$$

where δ_{Σ} - the error of the mutual orientation of the assembled part axes;

φ_{Σ} - the error of the mutual angular orientation of the assembled parts contours;

γ_{Σ} - the error of the mutual angular rotation of the assembled parts contours;

$[\delta_0]$, $[\varphi_0]$ и $[\gamma_0]$ - the acceptable error values.

The angular location accuracy of the mating parts towards the axis of the assembly is determined by the equation (3) (Pops & Lobzov, 1976).

$$[\gamma_0] = \frac{\pi}{n} \cdot \arccos \left[\frac{D}{d} \cdot \cos \frac{\pi}{n} \right] \quad (3)$$

где $[\gamma_0]$ – the permissible angular error of the parts position, mm

n – the number of faces on mating surfaces

D – the minimum diameter of the inscribed circle of the hole, mm

d – the maximum diameter of the circumscribed circle of the shaft, mm

The problem of robotic assembly was considered by many researchers. In particular, the application of high-frequency oscillations (up to 9000 Hz) for directional alignment of cylindrical and prismatic parts with and without chamfers is described in (Baksys & Kilikevicius, 2011), (Baksys, et al., 2017) and (Sadauskas & Baksys, 2013). In contrast to the present paper, the study object is press-fit joints, in which the base part has free location, and the shaft is fixed in a gripper with elastic elements. Vibrations from the piezoelectric generator are transmitted to the shaft in axial direction. The reliability of the assembly process was not studied. In this paper, the base part has a rigid base, and the vibrations are low-frequency and are induced relative to two mutually perpendicular horizontal axes. Thus, it makes possible to avoid jamming of parts.

In (Vartanov, et al., 2017) a method for robotic assembly of cylindrical joints using low-frequency vibrations and adaptive robot gripper was proposed (Vartanov, et al., 2010). This work is a development of the proposed method as applied to the assembly of profile shafts. In contrast to the previous method, an additional movement, namely a rotation around the vertical axis Z in order to align the profile of the shaft and the bush, is introduced into the vibration assembly device (fig. 30).

2. Mathematical model

Thus, the vibration assembly device is a three-link manipulator, each link of it being driven from a separate drive.

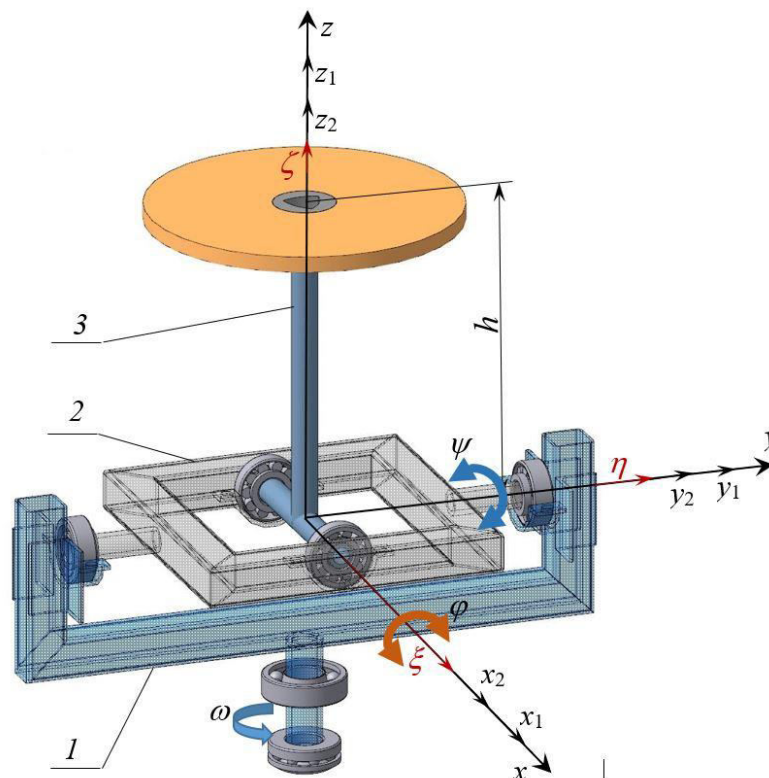


Fig 3. Kinematics of the assembly vibration device

For definiteness, we introduce a series of coordinate systems with a common starting point O: $Oxyz$ – fixed coordinate system;

$Ox_iy_iz_i$ ($i=1,2$) – the coordinate systems rigidly associated with the first and second link of the vibrating device respectively;

$O\xi\eta\zeta$ – the coordinate system rigidly associated with the third link of the device.

The vibrating disk is strictly connected to the third link of the device, in the center of which there is a holder with a bush rigidly fixed in it.

The cylindrical profile shaft is placed in the gripping device of the robot and has the possibility of elastic displacements in the vertical plane along two mutually perpendicular directions (in the direction of the axes C_4y_4 and C_4z_4). The coordinate system $C_4x_4y_4z_4$ is rigidly associated with the gripper, where the point C_4 is the mass center of the gripping device (fig. 4).

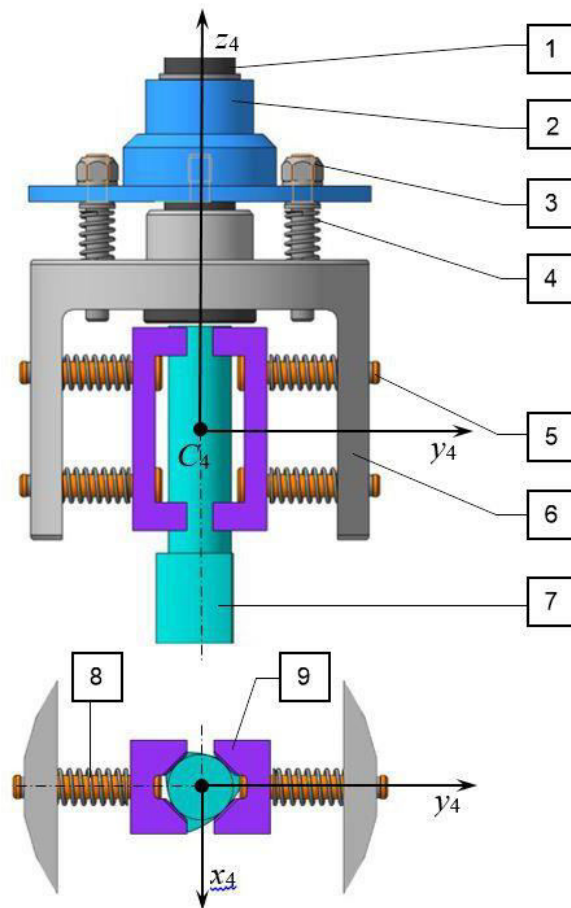


Fig.4. The mass center of the gripping device (the coordinate system $C_4x_4y_4z_4$): 1 – a rod; 2 – a flange; 3 – a stud; 4, 8 – a spring; 5 – a bolt; 6 – a casing; 7 – a part; 9 – a prismatic gripper

Consider the case when the initial contact of the shaft with the bush plane of the vibrating disk occurs at one point P (fig. 5). In this case, the angle of obliquity of the mating parts axes is assumed to be so small in the first approach that it can be neglected.

The coordinate system $C_5x_5y_5z_5$ is rigidly associated with the shaft. The origin of the system $C_5x_5y_5z_5$ coincides with the mass center of the shaft.

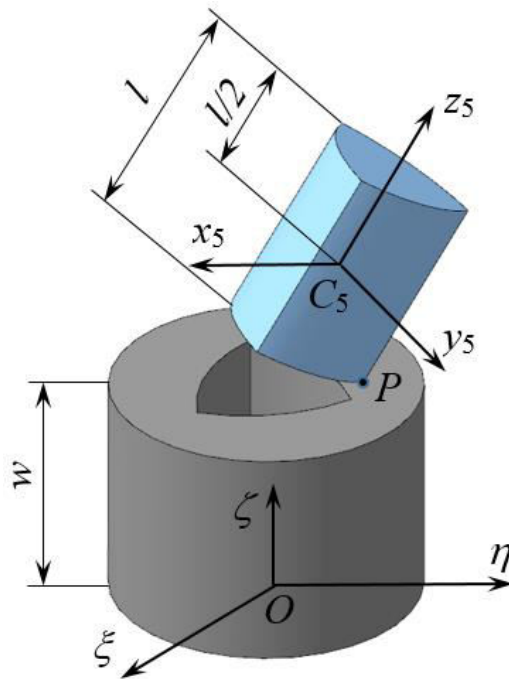


Fig.5. Kinematics of the initial contact of the profile shaft with the vibrating disk

The purpose of this article is to study the influence of oscillations and rotation of the first link of the assembly device on the movement type of the mass center of the profile part as well as the initial point of contact towards the bush, that is, towards the moving coordinate system $O\xi\eta\zeta$). It is also necessary to determine the effect of a number of parameters on the movement type of the part mass center towards the bush, namely: the height of the disk location of the vibration device "h" relative to the center of vibration; stiffness of the elastic elements of the gripping device (C_{41} - horizontal, C_{42} - vertical); the coefficient of friction between parts (f); the amplitude (A) and circular frequency (k) of oscillations of the second and third links of the device, as well as the magnitude of the angular rotation velocity of the first link of the assembly device (ω).

For this purpose, it is necessary to obtain differential equations of the mass center motion of the cylindrical part to the moving (non-inertial) coordinates $O\xi\eta\zeta$.

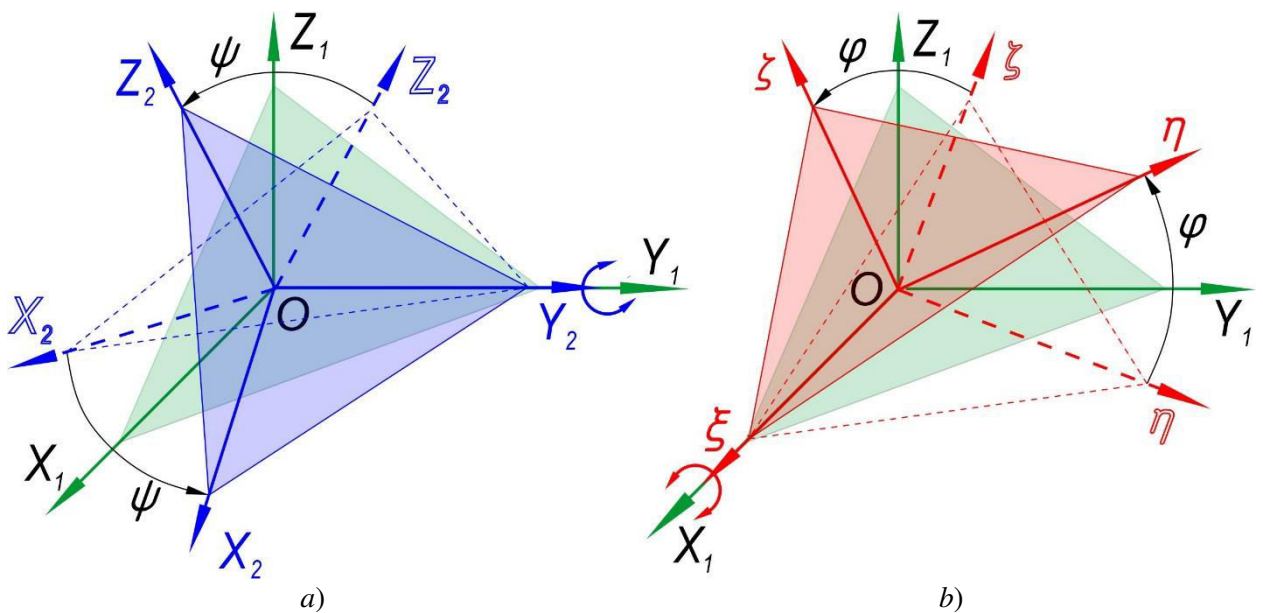


Fig.6. показать диапазон положений углов исправить на а) x_1 и x_2 , показать вращение вокруг y_1 и x_1 .

On the basis of the theorem on the mass center motion of the system (Dreizler & Lüdde, 2010) for the absolute motion of a cylindrical part provided that there is a contact with the surface of the vibrating disk, we obtain:

$$m\vec{a}_c = m\vec{g} + \vec{N} + \vec{F}_{fr} + \vec{F}_{el} + \vec{P}, \quad (4)$$

where:

m – the mass of the part;

\vec{a}_c - the absolute acceleration of the mass center of the part;

\vec{g} - the acceleration of gravity;

\vec{N} - the normal response of the vibrating disk plane;

\vec{F}_{fr} - the force of sliding friction;

\vec{F}_{el} - the resultant of elastic forces;

\vec{P} - the robot drive assembly force.

The absolute acceleration of the mass center of the cylindrical profile part based on the Coriolis theorem (Dreizler & Lüdde, 2010) can be represented as:

$$\vec{a}_c = \vec{a}_{cr} + \vec{a}_{ce} + \vec{a}_{ck}, \quad (5)$$

where \vec{a}_{cr} , \vec{a}_{ce} , \vec{a}_{ck} – the relative, transferable translational and Coriolis acceleration of the mass center of the part, respectively.

As a result of substituting (5) in (4), a differential equation of the relative motion of the part mass center (towards the sleeve) in vector form is obtained:

$$m\vec{a}_{cr} = m\vec{g} + \vec{N} + \vec{F}_{fr} + \vec{F}_{el} + \vec{F}_{ce} + \vec{F}_{ck} + \vec{P} \quad (6)$$

where \vec{F}_{ce} is the force of moving space;

\vec{F}_{ck} is the Coriolis force of inertia of the part mass center.

The transferable translational and Coriolis forces of the part mass center inertia are determined by the formulae, respectively:

$$\vec{F}_{ce} = -m\vec{a}_{ce} \quad (7)$$

$$\vec{F}_{ck} = -m\vec{a}_{ck} \quad (8)$$

The differential equation (4) is presented in the projections on the axis of the moving coordinates $O\xi\eta\zeta$, rigidly associated with the bush:

$$\begin{aligned} m\ddot{\xi}_c &= (m\vec{g})_{\xi} + F_{TP\xi} + F_{\xi}^{yn} + F_{ce\xi}^{un} + F_{ck\xi}^{un} + P_{\xi}, \\ m\ddot{\eta}_c &= (m\vec{g})_{\eta} + F_{TP\eta} + F_{\eta}^{yn} + F_{ce\eta}^{un} + F_{ck\eta}^{un} + P_{\eta}, \\ m\ddot{\zeta}_c &= (m\vec{g})_{\zeta} + F_{\zeta}^{yn} + F_{ce\zeta}^{un} + F_{ck\zeta}^{un} + N + P_{\zeta}. \end{aligned} \quad (9)$$

where

- ξ_c, η_c, ζ_c – the coordinates of the part mass center (point C_5) in the coordinates $O\xi\eta\zeta$.
- F_{TP} – the friction force in projections on the axis of the moving coordinates $O\xi\eta\zeta$
- F_{ξ}^{yn} – the elastic force of robot gripper elements in projections on the axis of the moving coordinates $O\xi\eta\zeta$
- $F_{ce\xi}^{uH}$ – the force of moving space in projections on the axis of the moving coordinates $O\xi\eta\zeta$
- $F_{ck\xi}^{uH}$ – the Coriolis force in projections on the axis of the moving coordinates $O\xi\eta\zeta$
- P – the assembly force in projections on the axis of the moving coordinates $O\xi\eta\zeta$

The mathematical model of the relative motion dynamics of the mass center of a cylindrical profile part if there is its single-point contact with the plane of the vibrating disk (with the plane of the bush) is as follows:

$$\begin{aligned}
 m\ddot{\xi}_c = & p \sin \psi - c(\xi_c + Z_{c4} \sin \psi) - fN \frac{\dot{\xi}_k}{\sqrt{\xi_k^2 + \eta_k^2}} + m(\xi_c \dot{\psi}^2 - \eta_c \dot{\psi} \sin \varphi - 2\eta_c \dot{\varphi} \dot{\psi} \cos \varphi - \\
 & - 2\eta_c \omega \dot{\varphi} \sin \varphi - \zeta_c \dot{\psi} \cos \varphi + 2\zeta_c \dot{\varphi} \dot{\psi} \sin \varphi - 2\zeta_c \omega \dot{\varphi} \cos \varphi \cos \psi + \xi_c \omega^2 \cos^2 \varphi + \\
 & + \eta_c \omega^2 \sin \psi \sin \varphi \cos \psi + \zeta_c \omega^2 \sin \psi \cos \varphi \cos \psi) - 2m\dot{\xi}_c (\dot{\psi} \cos \varphi + \omega \cos \psi \sin \varphi) + \\
 & + 2m\dot{\eta}_c (-\dot{\psi} \sin \varphi + \omega \cos \psi \cos \varphi); \\
 m\ddot{\eta}_c = & -p \cos \psi \sin \varphi - c(\eta_c - Z_{c4} \cos \psi \sin \varphi) - fN \frac{\dot{\eta}_k}{\sqrt{\xi_k^2 + \eta_k^2}} + m(\xi_c \dot{\psi} \sin \varphi + \eta_c \dot{\psi}^2 \sin^2 \varphi + \\
 & + \eta_c \dot{\varphi}^2 - 2\eta_c \omega \dot{\varphi} \sin \psi + \zeta_c \dot{\psi}^2 \cos \varphi \sin \varphi + \xi_c \omega^2 \sin \psi \cos \psi \sin \varphi + \zeta_c \dot{\varphi} + \\
 & + \eta_c \omega^2 \sin^2 \varphi \sin^2 \psi + \zeta_c \omega^2 \sin^2 \psi \sin \varphi \cos \varphi + 2\xi_c \omega \dot{\psi} \sin \psi \cos \varphi - \\
 & - 2\eta_c \omega \dot{\psi} \cos \psi \sin \varphi \cos \varphi - 2\zeta_c \omega \dot{\psi} \cos \psi \cos^2 \varphi + \eta_c \omega^2 \cos^2 \varphi - \zeta_c \omega^2 \sin \varphi \cos \varphi) - \\
 & - 2m\dot{\xi}_c (-\dot{\psi} \sin \varphi + \omega \cos \psi \cos \varphi) + 2m\dot{\zeta}_c (\dot{\varphi} - \omega \sin \psi);
 \end{aligned} \tag{10}$$

- where p – the assembly force;
- f – the friction coefficient between mating parts
- N – the normal response of the vibrating disk plane
- M – the mass of the part;
- C – stiffness of the elastic element in the robot gripper

Differential equations of the relative motion of the part mass center without its contact with the plane of the vibrating disk are given by:

$$\begin{aligned}
m\ddot{\xi}_c = & -c(\xi_c + Z_{c4} \sin \psi) + m[\xi_c \dot{\psi}^2 - \eta_c \ddot{\psi} \sin \varphi - 2\eta_c \dot{\varphi} \dot{\psi} \cos \varphi - \\
& - 2\eta_c \omega \dot{\varphi} \sin \varphi - \zeta_c \dot{\psi} \cos \varphi + 2\zeta_c \dot{\varphi} \dot{\psi} \sin \varphi - 2\zeta_c \omega \dot{\varphi} \cos \varphi \cos \psi + \\
& + \xi_c \omega^2 \cos^2 \psi + \eta_c \omega^2 \sin \psi \sin \varphi \cos \psi + \zeta_c \omega^2 \sin \psi \cos \varphi \cos \psi] - \\
& - 2m\zeta_c (\dot{\psi} \cos \varphi + \omega \cos \psi \sin \varphi) + 2m\eta_c (-\dot{\psi} \sin \varphi + \omega \cos \psi \cos \varphi) + p \sin \psi; \\
m\ddot{\eta}_c = & -c(\eta_c + Z_{c4} \cos \psi \sin \varphi) + m[\xi_c \dot{\psi} \sin \varphi + \eta_c \dot{\psi}^2 \sin^2 \varphi + \eta_c \dot{\varphi}^2 - \\
& - 2\eta_c \omega \dot{\varphi} \sin \psi + \zeta_c \dot{\psi}^2 \cos \varphi \sin \varphi + \zeta_c \omega^2 \sin \psi \cos \psi \sin \varphi + \\
& + \zeta_c \dot{\varphi} + \eta_c \omega^2 \sin^2 \psi \sin^2 \varphi + \zeta_c \omega^2 \sin^2 \psi \sin \varphi \cos \varphi + 2\xi_c \omega \dot{\psi} \sin \psi \cos \varphi - \\
& - 2\eta_c \omega \dot{\psi} \cos \psi \sin \varphi \cos \varphi - 2\zeta_c \omega \dot{\psi} \cos \psi \cos^2 \varphi + \eta_c \omega^2 \cos^2 \varphi - \\
& - \zeta_c \omega^2 \sin^2 \varphi \cos \varphi] - 2m\zeta_c (-\dot{\psi} \sin \varphi + \omega \cos \psi \cos \varphi) + 2m\zeta_c (\dot{\varphi} - \omega \sin \psi) - \\
& - p \cos \psi \sin \varphi; \\
m\ddot{\zeta}_c = & -c(\zeta_c - Z_{c4} \cos \psi \cos \varphi) + m[\xi_c \omega^2 \cos \psi \sin \psi \cos \varphi + \eta_c \omega^2 \sin^2 \psi \sin \varphi \cos \varphi - \\
& - \eta_c \omega^2 \sin \varphi \cos \varphi + \zeta_c \omega^2 \sin^2 \psi \cos^2 \varphi + \zeta_c \omega^2 \sin^2 \varphi - 2\zeta_c \omega \dot{\varphi} \sin \psi + \\
& + \xi_c \dot{\psi} \cos \varphi + \eta_c \dot{\psi}^2 \sin \varphi \cos \varphi - \eta_c \dot{\varphi} + \zeta_c \dot{\psi}^2 \cos^2 \varphi + \zeta_c \dot{\varphi}^2 - 2\xi_c \omega \dot{\psi} \sin \psi \sin \varphi + \\
& + 2\eta_c \omega \dot{\psi} \cos \psi \sin^2 \varphi + 2\zeta_c \omega \dot{\psi} \cos \psi \sin \varphi \cos \varphi] - 2m\eta_c (\dot{\varphi} - \omega \sin \psi) + \\
& + 2m\zeta_c (\dot{\psi} \cos \varphi + \omega \cos \psi \sin \varphi) - p \cos \psi \cos \varphi.
\end{aligned} \tag{11}$$

3. Simulating the robotic assembly

On the basis of the mathematical model, a program implementing the analytical solution of the equations obtained according to the given initial parameters was developed.

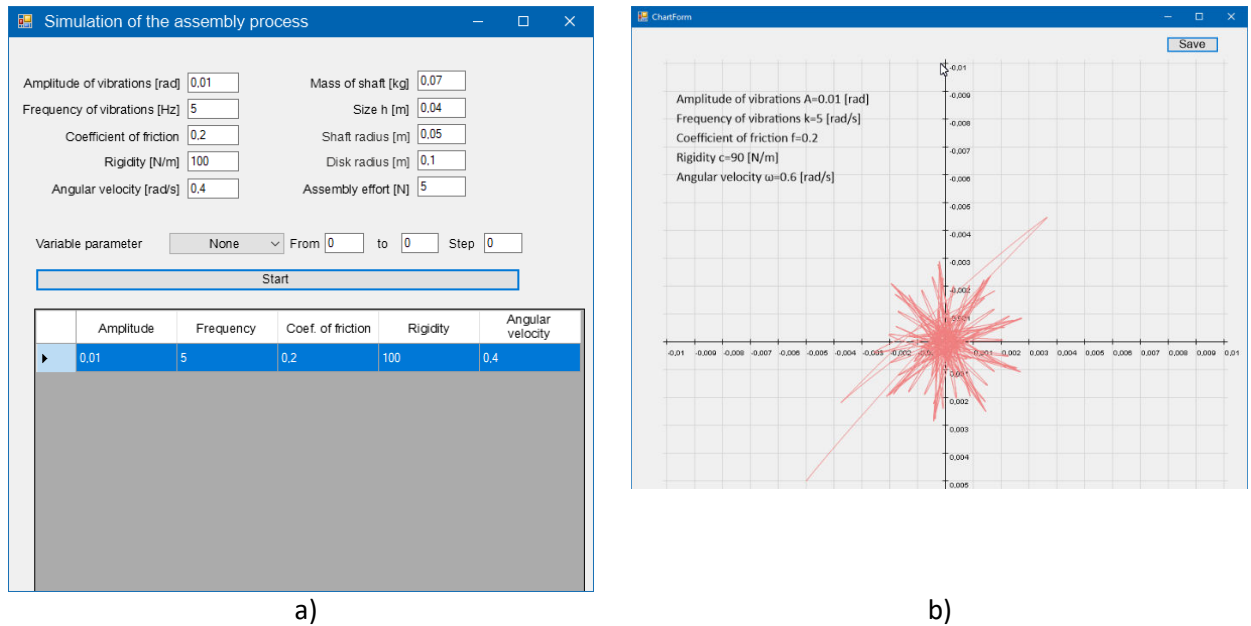


Fig. 7. Program for modeling the process of overlapping the mass center of assembled parts: a) program interface; b) the result of modeling

The result of the analytical solution of the mathematical model equation is the trajectory of the mass center of the installed shaft relative to the non-inertial coordinate system. Trajectories were considered to be reasonable when the center of the scanning zone was combined with the center of the coordinate system (рис .7b). When modeling, process efficiency was not taken into account.

The program for simulating the robotic assembly process of profile joints is designed to determine the range of dynamic and design parameters in which the mass center of the installed part (the shaft)

asymptotically approaches the axis of the installed part (the shaft), creating conditions for trouble-free assembly of profile joints.

Thus, the program allows to determine the range of technological parameters, in which there is a stable overlap of the mass centers of the assembled parts (fig.8).

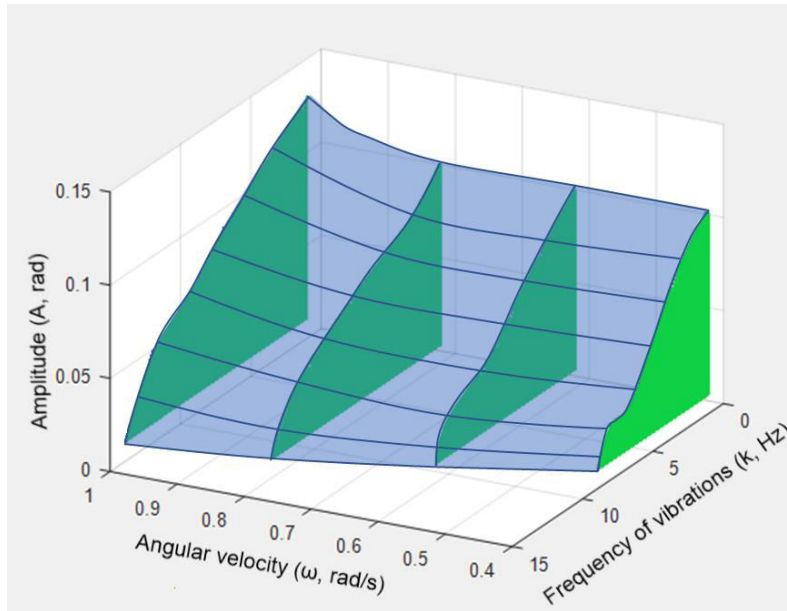


Fig. 8. Areas of stable alignment of mass centers of assembled parts

In the simulation, the following initial data were taken: the shaft mass — 0.13 kg; the shaft radius - 0.005 m; the shaft height - 0.1 m; the distance from the vibration center to the support surface h - 0.04 m.

The analysis of the computer modeling results shows that there is a region of oscillation amplitude at which a steady movement of the shaft mass center in the direction of the bush axis is observed. In modeling, this region arises from small amplitude values (0.01 to 0.1 rad) (fig. 9).

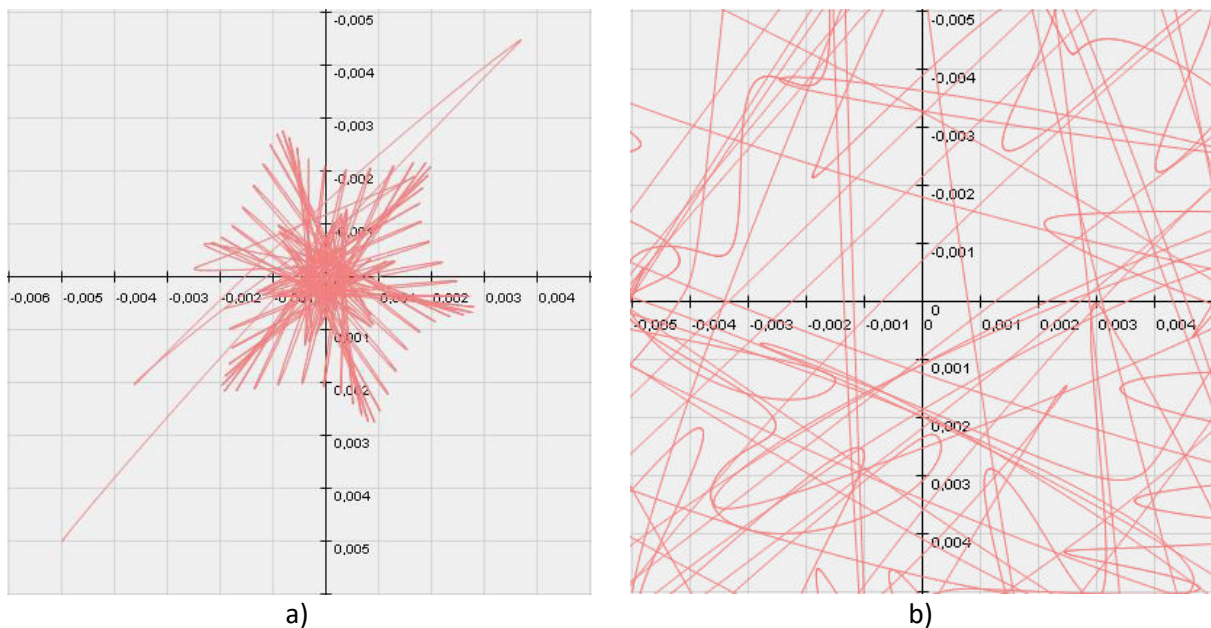


Fig. 9. Movement trajectories of the shaft mass center under the oscillation amplitude changes (constant values: frequency 3 Hz, coefficient of friction 0.2, rigidity 90 N / m, angular velocity 0.6 rad/s): a) amplitude 0.01 rad; b) amplitude 0.13 rad (x10e4 mm)

The frequency variations at which the shaft mass center asymptotically approaches the axis of the base part are from 1 to 15 Hz. When it is further increased, no change is observed in the process.

With an increase in the frequency of oscillations, a decrease in variations of the amplitude range is observed, whereby the process of overlapping the part mass centers is performed (fig. 8).

To exclude the possibility of mating parts impact against each other in the process of relative orientation, it is advisable to use a low angular velocity for alignment of the assembled part axes. The optimal value of the angular velocity is in the range (0.4-1 rad / s). When it goes beyond the specified limit, the parts mating does not occur. With an increase in the angular velocity of more than 1 rad / s, the effect of centrifugal force on the process of parts overlapping manifests itself. This eliminates the overlapping of part mass centers.

The analysis of the friction coefficient variations showed its insignificant influence on the movement trajectory of parts.

The analysis of the alignment trajectories shows (Fig. 8) that there is the rigidity range of elastic elements (from 30 N / m to 75 N / m and over 100 N / m), when the movement of the mass center of the attached part does not result in parts overlapping. In the range from 80 N / m to 100 N / m there is a steady approach of the installed part axis to the base one.

The assembly force range was from 1 N to 10 N. As shown by the simulation results, increasing the assembly force had a positive effect on the assembly process. At its low values (fig. 7a), no asymptotic movement was observed, since the mass center of the installed part passed through the axis of the base part, but when increasing (fig. 7b), optimal trajectories appeared.

The simulation confirmed that there is a dynamic parameter range (amplitude, frequency, angular velocity) and spring rigidity of the gripper, when the mass center of the attached part quickly approaches the axis of the base part. The analysis of the results shows that the process is more efficient with the following parameters: the amplitude of oscillations $A=0.005$ rad; the frequency of oscillations $K=12$ rad/s; the rigidity of the elastic elements of the adaptive gripper - $80 \div 100$ N/m; the angular velocity $\omega=0.03$ rad/s and the assembly force $P=6 \div 10$ N.

To verify the adequacy of the results obtained during modeling to the overlap conditions of the profile part contours, a physical experiment was conducted, taking into account the found values of technological parameters.

4. Description of the experimental device and experimental conditions

The design of the experimental device (fig. 10 and fig.11) for robotic assembly of profile joints provides a wide range of parameters and has tools to control the assembly process.

The design and functional features of the experimental device allow us to change the following parameters:

K – the oscillation frequency of the vibrating disk (5 ... 15 Hz);

A – the linear oscillation amplitude of the output link (vibrating disk) (0 ... 4 mm);

δ – the range of the linear misalignment of the assembled parts (0 - 2 mm);

ω – the rotation speed of the vibrating disk (0 ... 22 rpm).

The installed shaft is held by the adaptive gripper of the robot 2. The bush is installed in the center of the vibrating disk 4. Vibrations are generated by the low-frequency oscillator 5. The oscillation frequency is controlled with an electronic frequency meter 6, and the actual amplitude of oscillation is

monitored by contactless laser sensors 3. All signals are collected and processed by a computer. The vibrating disk driven from the electric motor rotates with a constant angular velocity ω .

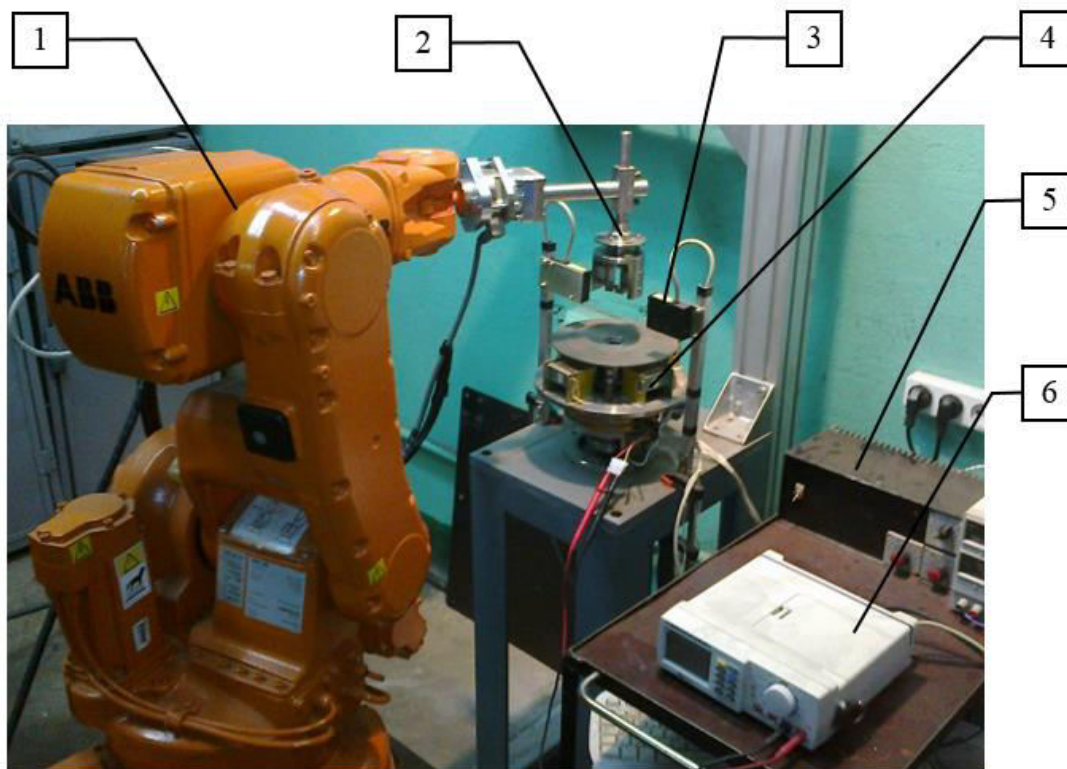


Fig. 10. The experimental device: 1) robot ABB IRB140, 2) the adaptive grip, 3) the contactless laser sensors, 4) the vibration device, 5) the low-frequency oscillator 6) the electronic frequency meter

After setting the required oscillation mode, the robot moved the shaft to the assembly zone with a given linear misalignment of parts. There was a contact between the shaft and the vibrating disk, resulting in alignment of parts under the influence of oscillations and the assembly force.

The parts mating was carried out according to the fit H8/f7 (ISO 286-1:2010) which involves the size of the gap from 13 to 50 μm .

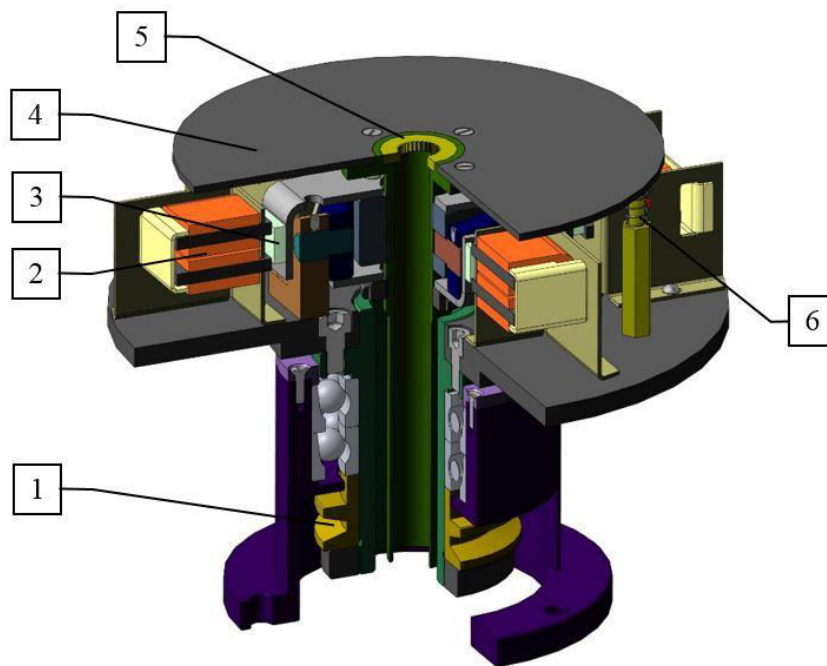


Fig. 11. Vibration device design:1) the V-belt pulley wheel, 2) the electromagnet, 3) the permanent magnet, 4) the vibrating disk, 5) the base part (bush), 6) damper springs.

The assembly process of profile joints was controlled by the following parameters: the oscillation amplitude, the oscillation frequency, the rotation speed of the vibrating disk and the assembly time.

To control the amplitude of oscillations in the experimental device, triangulation laser sensors Riftek RF603 X/10 were used, one for each axis of oscillations.

To control the oscillation frequency with an accuracy of 0.1 Hz, the electronic frequency meter – a digital multimeter Mastech M9803R was used.

The process and the completion of the assembly were monitored by changing the amplitude of oscillations controlled by the sensors.

5. Discussion of results

During the experiments a decrease in the oscillation amplitude of the vibrating disk was observed as the magnitude of parts mating (q) increased.

Experimental studies for evaluating the effect of the number of faces on the time of parts mating were conducted. The assembly time was found to decrease with the increasing number of faces. So, the assembly time for a triangular shaft is 3.3 sec, for tetrahedral one is 3.1 sec and for hex is 3 sec (fig. 12).

A series of experiments were conducted in compliance with the assemblability conditions of profile joints (conditions 2). The analysis of the results shows that using the proposed method ensures the assembly process without jamming. In order to avoid jamming conditions due to angular misalignments of parts, low frequency oscillations of the support were generated in the assembly zone. They were controlled by laser triangulation sensors (fig. 10). Low frequency oscillations had a linear amplitude of up to 4 mm and a frequency from 5 to 15 Hz.

In the numerical experiment, a positive effect of increasing the spring stiffness to a certain value was observed. When it increases, the loss of trajectory stability and, as a consequence, the increase in the assembly time due to the change in the trajectory type is found. The physical experiment confirmed the influence of the spring stiffness of the robot gripper during the assembly time. The stiffness value (90 N/mm) was set to ensure minimum assembly time for any number of part faces.

At small values of the gripper spring stiffness (less than 80 N / mm) there is no effect of relative centering of the assembled parts due to a small magnitude of the elastic force. If the values are over 110 N/mm the spring stiffness prevents the effect of the relative centering, since the elastic force F^{el} is much higher than the force of moving space F_{ce}^{in} .

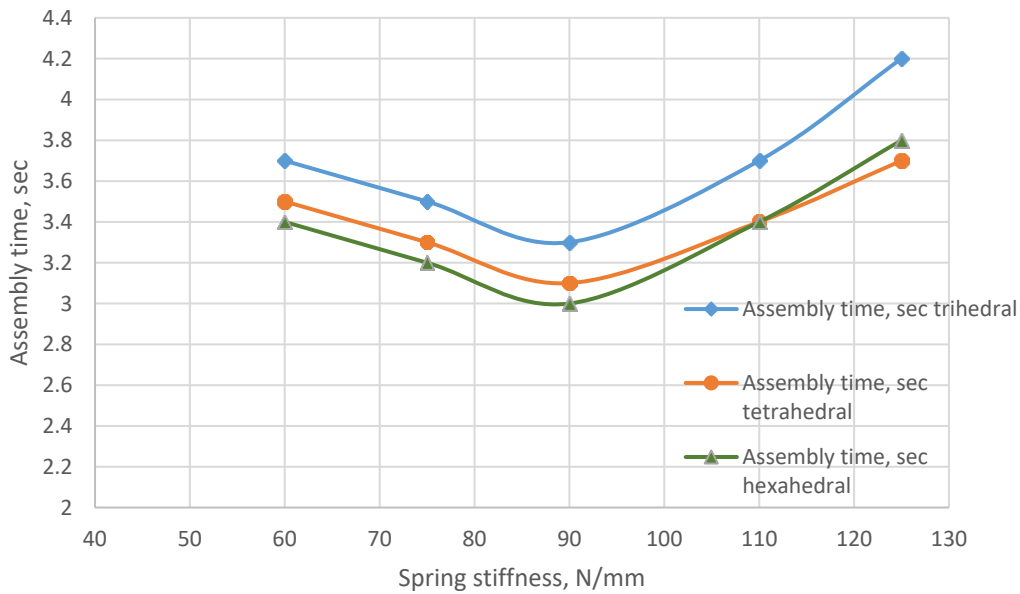


Fig.12. Effect of the spring stiffness on the assembly time

During the experiments, the influence of the angular velocity of the disk rotation on the assembly time was studied. The positive effect of increasing the angular velocity to a certain value was found. Then with its further increase the loss of stability and an increase of the assembly time were revealed. It indicates inertia effect. This effect is due to the misalignment of the assembly linear speed and the rotation relative to the assembly axis. Fig. 13 presents the experimental results for trihedral parts. In the case of a greater number of part faces the effect occurred to a greater extent.

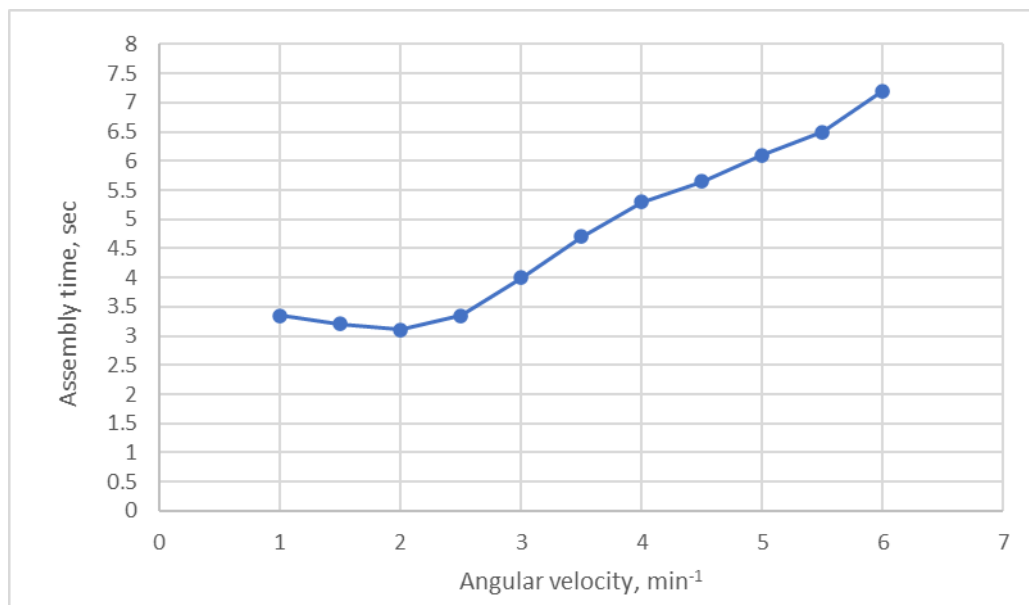


Fig. 13. Effect of the angular velocity on the assembly time

The influence of the oscillation amplitude of the vibrating disk on the assembly time of the parts is studied. The dependence is found to be extreme (Fig.) due to the inertia effect of the process.

The dependence of the assembly time on the oscillation frequency is also revealed. This dependence (Fig.) is a curve with saturation. At frequencies greater than 12 Hz, the assembly time does not change.

Studies of the influence of the oscillation amplitude on the assembly time of parts were carried out. The dependence was found to be extreme (Fig. 14) due to the inertia effect of the process. When the amplitude is more than 1 mm, the phenomenon of a part bounce from the support surface begins, resulting in an unstable nature of the movement of the oriented part.

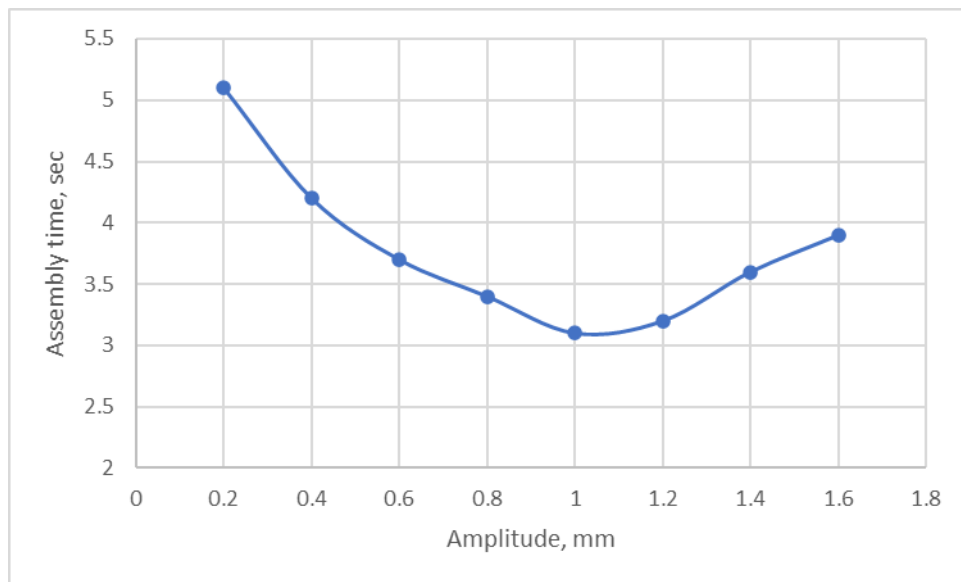


Fig. 14. Influence of the oscillation amplitude on the assembly time

The dependence of the assembly time on the oscillation frequency was also revealed. This dependence (Fig. 15) has the character of an asymptotic curve. The assembly time does not change at frequencies more than 12 Hz.

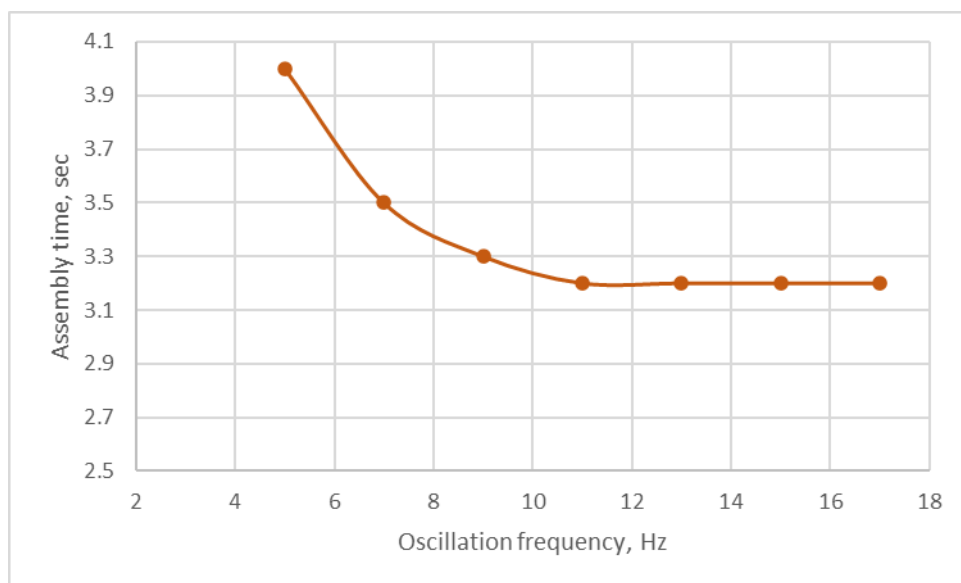


Fig. 15. Dependence of the assembly time on the oscillation frequency

According to the found values of technological parameters 100% assemblability of parts was ensured.

6. Conclusion

A method of robotic assembly of profile joints using adaptation tools is proposed, which ensures an efficient assembly process of the profile faceless joints with a gap of up to 0.01 mm.

A mathematical model of the dynamics of the mass center movement of the installed profile part in relation to the non-inertial coordinate system rigidly connected with the rotating and vibrating base part was developed.

On the basis of the proposed mathematical model of dynamics the computer simulation of the process was carried out. The results shows that there are technological and design parameters ranges (oscillation amplitudes A -0,5...1,2 mm, oscillation frequency K -10...15 Hz, the stiffness of the elastic elements of the gripper c -80 ... 90 N/mm, angular velocity ω -1...2 rpm, P -6...10 N), whereby the alignment of assembled parts axes is fast and stable.

The simulation and physical experiments confirmed an expected effect. The result analysis of theoretical and experimental studies using a device for compensating errors in the robot positioning during the profile joint assembly shows that the method provides the reliable assembly with linear errors up to 2 mm and angular position errors up to $1^{\circ}50'$. The given values were selected as the maximum acceptable for robotic assembly. They are summarized taking into account errors of the robot positioning, technological equipment, transport system and locating.

The assumption of improving the assembly reliability when applying the adaptive gripper and oscillations that exclude jamming of the assembled parts is confirmed. It is experimentally found that under the conditions of profile joint assemblability, the relative orientation process of profile shafts using the adaptation tools is 1.5 seconds faster than without their application. However, in case of non-compliance with the assemblability, using adaptation tools showed the same results with a slight increase of the parts mating time, but without them 100% jamming was observed.

It is experimentally established that the greater the number of faces of the assembled parts, the shorter the time of their alignment. This is due to the fact that the large number of faces reduces the rotation angle to align the mating surfaces.

Acknowledgment

The authors express their gratitude to the head of the department laboratory "Technologies and equipment of mechanical engineering" Mishin Vladimir Nikolaevich for helpful advice and assistance in conducting experimental research. Experimental research has become possible due to the participation of company "Rubin" in the retrofitting of the experimental installation.

Declarations

- Funding: Not applicable
- Conflict of interest/Competing interests: The authors declare no conflict of interest.
- Ethics approval: Not applicable
- Consent to participate: Not applicable
- Consent for publication: Not applicable
- Availability of data and materials: Not applicable
- Code availability: Not applicable
- Authors' contribution: Not applicable

References

- [1] The application of this method ensures the technological reliability of the robotic assembly of the RK-profile joints (Vartanov, et al., 2012).
- [2] Baksys, B., Baskutiene, J. & Baskutis, S., 2017. The vibratory alignment of the parts in robotic assembly. *Industrial Robot*, 44(6), pp. 720-729.
- [3] Baksys, B. & Kilikevicius, S., 2011. *Vibration Problems ICOVP*. s.l., s.n.
- [4] Dreizler, R. M. & Lüdde, C. S., 2010. *Theoretical Mechanics. Theoretical Physics 1*. Berlin, Heidelberg: Springer.
- [5] Karelin, N., 1966. *Non-copied processing of cylindrical parts*. Moscow: Mashinostroenie.
- [6] Mossdorf, R. / E. K. & C. A. G., 1938. *Production of cross-section profiles bounded by cycloidal curves*. USA, Patent No. US2267250 A.
- [7] Musyl, R., 1946. Das K- Profil eine zyklische Kurve. *Maschinenbau und Wärmewirtschaft*, Issue 1, pp. 100-102.
- [8] Musyl, R. D.-I. & Danzer, F. D.-I., 1941. *Verfahren und Vorrichtung zum rein getriebemaessigen Herstellen, insbesondere durch Schleifen, von unruunden Querschnitten an Aussen- und Innenprofilen*. Germany, Patent No. DE 759350 C.
- [9] Pops, J. K. & Lobzov, B. A., 1976. Determination of conditions for automatic assembly of non-cylindrical parts. *Automation of assembly processes*, 10 05, Issue 5, pp. 36-44.
- [10] Sadauskas, E. & Baksys, B., 2013. Alignment of the parts using high frequency vibrations. *Mechanika*, 19(2), pp. 184-190.
- [11] Timchenko, A., 1993. *Processes for forming the profile surfaces of products with an equiaxial contour (Diss. Dr. of Tech. Sc.)*, Moscow: s.n.
- [12] Vartanov, M. V., Bojkova, L. V. & Bakena Mbua, J. K., 2012. *The method of assembly of profile joints with a gap*. RU, Patent No. 4445200.
- [13] Vartanov, M. V., Bojkova, L. V. & Kolchugin, I., 2010. *Assembly method for shaft – bush connections*. Russian Federation, Patent No. 2381095.
- [14] Vartanov, M. V., Bojkova, L. V. & Zinina, I. N., 2017. Mathematical model of robotic assembly by means of adaptation. *Assembly Automation*, 37(1), pp. 130-134.